Journal of Structural Chemistry. Vol. 58, No. 6, pp. 1061-1068, 2017.

PHOTOELECTRON SPECTRA AND ELECTRONIC STRUCTURE OF AZA-BORON-DIPYRIDOMETHENE DERIVATIVES

S. A. Tikhonov[1], V. I. Vovna[1], and A. V. Borisenko[2]

UDC 544.15:544.17:544.18

The electronic structure of three aza-boron-dipyridomethene derivatives containing different hydrocarbon groups at the boron atom is studied by ultraviolet photoelectron spectroscopy and calculations at the density functional theory level. According to the experimental and theoretical data, the higher occupied molecular orbitals of anthracene, acridine, and the studied complexes are of the same character. For the three studied compounds, the effect of alkyl and phenyl substituents on the electronic structure is determined. The parameters of the electronic structure of aza-boron-dipyridomethene (phenyl groups at the boron atom) and its β-diketonate analogue are compared. It is shown that in an energy range up to 11 eV the calculated results correlate with the ultraviolet photoelectron spectra.

DOI: 10.1134/S0022476617060026

Keywords: electronic structure, photoelectron spectroscopy, density functional theory, chelates, boron complexes, aza-boron-dipyridomethylene.

INTRODUCTION

Chelate boron complexes have important physicochemical properties. In particular, boron β-diketonates exhibit intensive luminescence [1], liquid crystalline properties [2], high biological activity [3] and find their application as optical materials [4] and antivirals [5]. No less relevant are the investigations of the optical properties of nitrogen-containing analogues of boron β-diketonates [6]. Nitrogen-containing boron complexes with condensed rings attract the researchers' attention. A set of specific properties and luminescence [7, 8] of boron dipyrido (BODIPY) methylene and its derivatives determine the promising use of BODIPY-based materials as laser dyes [9], active components of solar collectors [10], biomolecular markers [11], and optical chemosensors [12]. Yet, most BODIPY dyes have a small Stokes shift (<10 nm). The materials based on aza-boron-dipyridomethene derivatives have noticeably larger Stokes shifts [13], which extends their potential application.

The establishment of relationships between the functional characteristics of the substances and their electronic structures opens the ways for the directed synthesis of novel luminophores. The works examining the optical properties of BODIPY derivatives employ the experimental techniques of luminescent spectroscopy [7, 12] and absorption spectroscopy [14, 15]. The density functional theory (DFT) and time-dependent DFT are the most popular computational methods.

[1]Far Eastern Federal University, Vladivostok, Russia; allser@bk.ru. [2]Russian Customs Academy, Vladivostok Branch, Vladivostok, Russia. Translated from *Zhurnal Strukturnoi Khimii*, Vol. 58, No. 6, pp. 1107-1114, July-August, 2017. Original article submitted August 4, 2016.

However, at present, there are no works studying the electronic structure of substituted aza-boron-dipyridomethene by ultraviolet photoelectron spectroscopy (UPS).

As we have shown in [16, 17], the calculations at the DFT level allow the estimation of ionization energies (IEs) of nitrogen-containing boron complexes with an accuracy up to 0.1 eV. Good coincidence between the theoretical and experimental data enables the analysis of the structure of valence electronic levels and the unambiguous interpretation of the UPS spectra. This work reports the results of the investigation of the electronic structure of three of aza-boron-dipyridomethene derivatives **I–III** from the UPS and DFT data.

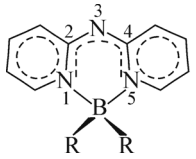

I R = C_2H_5
II R = C_3H_7
III R = C_6H_5

EXPERIMENTAL AND COMPUTATIONAL TECHNIQUES

The samples were synthesized at the Zelinsky Institute of Organic Chemistry, Russian Academy of Sciences, according to the procedures described in [18]. The UPS spectra of vapor of compounds **I–III** were recorded on a modified ES-3201 electron spectrometer with a monochromatic He I radiation source ($h\nu$ = 21.2 eV). A determination error of the band peaks did not exceed 0.02 eV. The temperature of the ionization cuvette depended on the vapor sublimation temperature of a certain sample and ranged from 180 °C to 240 °C. All UPS spectra have bands in a range from 7 eV to 11 eV. It is impossible to interpret the spectra in an energy range above 11 eV. Due to destructive phenomena in obtaining of compound **Ia** vapor (R=F) we failed to measure its UPS spectrum.

The spectra were interpreted using the results of the electronic structure modeling. The computational technique was chosen based on the analogy between the quasi-particle Dyson equation and the Kohn–Sham (KS) equation. The general Dyson equation [19] is one of the ways to derive the Green functions [20]. In [21, 22], it was shown that KS orbitals could serve as a good approximation to Dyson orbitals in the valence band. This explains good correlation between the experimental and theoretical IEs [23-25].

The DFT calculations were made using the Firefly 8.1.G software [26] with the TZVPP basis set [27]. For the quantum chemical calculations of the boron complexes [28-30] the hybrid three-parameter B3LYP functional has been successfully applied [31]. In this work and in [16, 17, 23-25] we performed the calculations with the B3LYP functional. This enabled us to exclude the functional influence on the electronic substitution effects.

Based on the calculated data, the regularities of the UPS spectra of the studied compounds were analyzed, which provided a guide for the band assignment. In the comparison of the experimental ionization energies (IE_i) with the calculated electron energies ε_i the procedure analogous to the Koopmans theorem ($IE_i = -\varepsilon_i + \delta_i$) was used, where δ_i was the orbital energy correction.

The UPS spectral bands corresponding to several orbitals were fitted with Gaussians. In the Gaussian fitting of the spectral bands, the number of calculated electronic levels, energy gaps between them, and the similarity of the ionization cross-sections were taken into account. The Gaussian peak energies IE_g were taken for IE_i values.

RESULTS AND DISCUSSION

The calculated interatomic distances and bond angles for **I–III** together with the respective data for ionized complex $\mathbf{I}^+$ are presented in Table 1.

TABLE 1. Geometric Parameters of Compounds **I**–**III** and $\mathbf{I}^+$

Bond	**I**	**II**	**III**	$\mathbf{I}^+$	Angle	**I**	**II**	**III**	$\mathbf{I}^+$
	R_{AB}, Å					Angle, deg			
B–C	1.64	1.64	1.68	1.75	C–B–C	117	117	115	100
B–N	1.62	1.62	1.63	1.52	N1–B–N5	105	105	104	111
N1–C2	1.37	1.37	1.38	1.42	B–N1–C2	123	123	123	121
C2–N3	1.33	1.33	1.33	1.33	C2–N3–C4	122	122	122	123

The optimization of the geometric parameters of complexes **I** and **II** in the starting symmetrical geometry (symmetry group C_2) gave the minimum energy when the alkyl groups were located on either side of the plane perpendicular to the chelate ring. The structure of **III** corresponds to symmetry group C_{2v}, and the phenyl groups are arranged as in the boron β-diketonate analogue $(C_6H_5)_2$BAcac [32]. There are no marked differences in bond lengths and bond angles in the chelate ring in a series of the studied complexes. However, the structural parameters of the first coordination sphere of complex **III** slightly differ from the analogous characteristics of compounds **I** and **II** (Table 1).

In the text and tables, the preferred localization of molecular orbitals (MOs) and effective charges are denoted by the following indices: *a* for the localization on the $C_{10}N_3H_8$ ligand; *b* for the localization on complexing agents F_2B, $(C_2H_5)_2B$, $(C_3H_7)_2B$, $(C_6H_6)_2B$. The MOs of complexes **I–II** and **III** were classified by the symmetry type using the irreducible representations of the C_2 and C_{2v} groups respectively. For BC_2 bonding orbitals (σ) of compounds **I–II** the C_s local symmetry relative to the chelate ligand plane was used.

The effective charges and the B–N and B–C bond orders in Table 2 show the effect of substituents R on the electron density distribution and the covalent bonding in the series of complexes **I–III**, as well as ionic $\mathbf{I}^+$ and **Ia** (R=F). In the NBO approximation, the total negative charges on R_2 noticeably exceed the charges on *a*. However, a high negative charge of two nitrogen atoms (–0.98 *e* …–0.99 *e*), which is mainly due to carbonyl carbon atoms C2 and C4, provides the high ionicity of boron bonds with ligand *a*. Compounds **I–III** and **Ia** are observed to have similar charges of the complexing agent (+0.13 *e*…+0.14 *e*); and the nitrogen atoms withdraw the electron density from carbon atoms C2 and C4 (+0.82 *e*), causing the field effect on the lone pair of nitrogen atom N3. The B–C bond orders in complex **III** are less and the B–N bond orders are greater than in **I–II**. The fluorine substitution for hydrocarbon groups in **I–III** (complex **Ia**) increases the bond orders in the first coordination sphere by 20% (Table 2).

As a result of the nuclear core relaxation in compound **I**, which is caused by an electron removal from the highest occupied molecular orbital (HOMO) π_7, the B–C and N1–C2 bond lengths increase by 0.11 Å and 0.05 Å (Table 1). The B–N bond lengths decrease by 0.10 Å. As for the bond angles, those in the first coordination sphere are changed the most (Table 1). Following the Franck–Condon principle, substantial changes in the equilibrium coordinates of the stretching and bending vibrations in ion $\mathbf{I}^+$ cause an increase in the vertical transition energy by 0.44 eV as compared to IE_{ad}. The electron relaxation in the ion leads to a decrease in the electron density on all atoms of the complex, yet the greatest change is observed for the C_2H_5 substituents (Table 2).

TABLE 2. Total Effective NBO Charges (e) of the Complexing Agent and the Chelate Ligand, Bond Orders of the First Coordination Sphere in Compounds **I**–**III**, $\mathbf{I}^+$ and **Ia**

Compound	Effective charge			Bond orders		Compound	Effective charge			Bond orders	
	B	R_2	*A*	B–N	B–C/B–F		B	R_2	*A*	B–N	B–C/B–F
Ia	+1.14	–1.01	–0.13	0.80	1.16	**II**	+0.72	–0.58	–0.14	0.65	0.94
$\mathbf{I}^+$	+0.83	+0.08	+0.09	0.88	0.72	**III**	+0.69	–0.57	–0.12	0.71	0.83
I	+0.71	–0.57	–0.14	0.65	0.96						

The structures of **I–III** have the π-system isoelectronic to that of the anthracene molecule. In order to determine the effect of the complexing agent on the electronic structure of the complexes, we analyzed the changes in the calculated electron energies and the MO characters on passing from anthracene and acridine to **Ia** and **I–III** (Fig. 1, Table 3). The anthracene, acridine, **Ia**, and **I–III** molecules are characterized by the presence of seven occupied π orbitals; and their HOMO is localized on three rings (Figs. 1 and 2). The field effect of two carbonyl carbon atoms (C2 and C4) in **Ia** and **I–III** stabilizes level n_N as compared to the respective value for the acridine molecule (Fig. 1), which causes an increase in the energy gap between the π_7 and n_N MO levels. The anthracene π_3 and acridine π_4 orbitals correlate with the π_4 MOs of complexes **Ia** and **I–II** (Fig. 1). As opposed to complex **Ia**, the mixing of π orbitals of the chelate ligand and pseudo-π MOs of the complexing agent σ″ and a_1^- is observed for compounds **I–III** (Figs. 1 and 2, Table 3).

There are no noticeable differences in the energies and compositions of six HOMOs for complexes **I** and **II** (Fig. 1, Table 3). However, on passing from **I** to **II** the contribution of the substituent orbitals to HOMO-6 increases and the HOMO-7 and HOMO-8 levels are destabilized (Fig. 1).

To find out the effect of the chelate ligand on the MO energies and composition, we analyzed the changes in the electronic structure on passing from compound **III** to $(C_6H_5)_2$BAcac (**IIIa**) [32]. The MOs of two C_6H_5 groups in complexes **III** (Table 3) and **IIIa** were classified using symmetry types C_{2v} of compounds **III** and **IIIa** and the local symmetry of the C_6H_5 and $(C_6H_5)_2$ substituents (Table 4).

The presence of phenyl groups at the boron atom (complex **III**) stabilizes the MO energies of the chelate ligand by 0.1-0.2 eV (Fig. 1, Table 3). The energy stabilization of the σ″–π level localized more on the BC_2 fragment is 0.7 eV.

In complex **III**, as opposed to **IIIa**, HOMO is localized mainly on the chelate ligand (Table 3, Fig. 1). The following four orbitals of the phenyl groups in **III** correlate with the four higher occupied orbitals in **IIIa** (Fig. 1, Table 2); the energy stabilization is 0.2-0.4 eV, which can be explained by the effect of the π_3–a_1^- MO in **IIIa** (Fig. 1).

Fig. 3 depicts the UPS spectra (bold lines) of compounds **I–III** fitted with Gaussians (thin lines). When plotting the orbital energies (vertical lines) on the experimental spectra, the scale of calculated ε values was shifted relative to IE by averaged value δ_{av}. To determine the effect of the complexing agent on the electronic structure, Fig. 3 depicts the UPS spectra

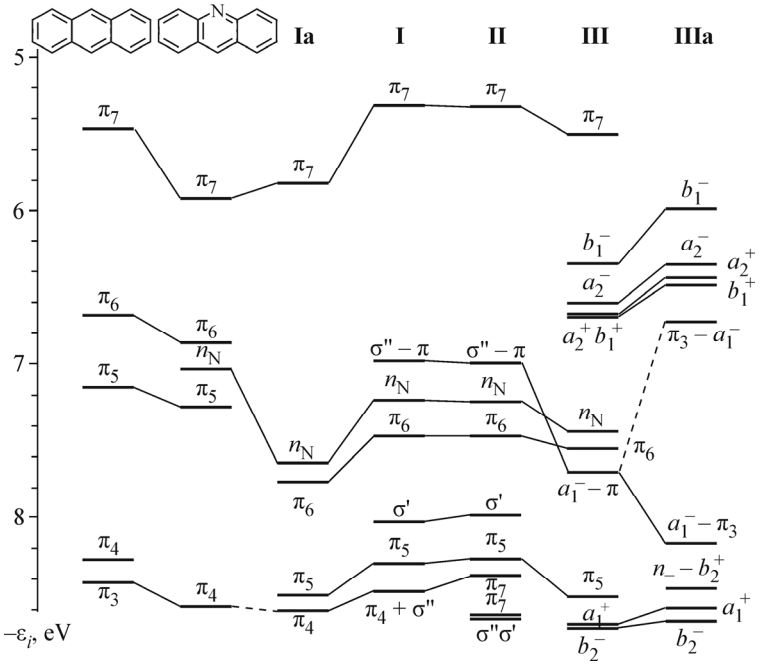

Fig. 1. Correlation chart of the higher occupied π and σ MOs of anthracene, acridine, **Ia**, **IIIa**, and compounds **I–III**.

TABLE 3. Characters and Symmetry of MOs, Electron Density Localization (%), Experimental and Calculated IEs (eV) of Compounds **Ia** and **I**–**III**

Symmetry, character (MO)	MO contributions		$-\varepsilon_i$	IE_g	δ_i
	b	*a*			
		Compound **Ia**			
HOMO, b_1 (π_7)	2	98	5.82	–	–
HOMO-1, a_1 (n_N)	0	100	7.64	–	–
HOMO-2, a_2 (π_6)	1	99	7.76	–	–
HOMO-3, a_2 (π_5)	8	92	8.51	–	–
HOMO-4, b_1 (π_4)	13	87	8.61	–	–
		Compound **I**			
HOMO, *b* (π_7)	9	91	5.31	7.11; 7.25	
HOMO-1, *b* (σ''–π)	70	30	6.98	9.09	2.11
HOMO-2, *a* (n_N)	6	94	7.23	9.33	2.10
HOMO-3, *a* (π_6)	1	99	7.47	9.58	2.11
HOMO-4, *a* (σ')	76	24	8.02	10.07	2.05
HOMO-5, *a* (π_5)	8	92	8.30	10.26	1.96
HOMO-6, *b* ($\pi_4 + \sigma''$)	38	62	8.48	10.51	2.03
		Compound **II**			
HOMO, *b* (π_7)	8	92	5.33	7.05; 7.25; 7.25	
HOMO-1, *b* (σ''–π)	70	30	6.99	8.87	1.88
HOMO-2, *a* (n_N)	6	94	7.24	9.24	2.00
HOMO-3, *a* (π_6)	1	99	7.48	9.49	2.01
		Compound **III**			
HOMO, b_1 (π_7)	7	93	5.50	7.16; 7.34	
HOMO-1, b_1 (b_1^-)	100	0	6.34	8.47	2.13
HOMO-2, a_2 (a_2^-)	99	1	6.60	8.67	2.07
HOMO-3, b_2 (a_2^+)	99	1	6.67	8.87	2.20
HOMO-4, a_1 (b_1^+)	95	5	6.68	8.88	2.20
HOMO-5, a_1 (n_N)	3	97	7.44	9.45	2.01
HOMO-6, a_2 (π_6)	5	95	7.55	9.56	2.01
HOMO-7, b_1 (a_1^-–π)	55	45	7.70	9.83	2.13

of the anthracene and acridine molecules. For the unambiguous interpretation of the UPS spectrum of **III**, the respective spectrum of **IIIa** is shown.

The presence of a fine structure of the first bands in the UPS spectra of compounds **I–III** whose π system is isoelectronic to that of the anthracene and acridine molecules (their spectra are observed to have a fine structure) is due to C=C π_7 bonding MO localized on three rings (Figs. 2 and 3). When moving from anthracene and acridine to **I–III** the IE_1 values change in accordance with the calculated data (Figs. 1 and 3). The stabilization of the experimental energies of the π_6 and π_5 MOs is also observed on passing from anthracene to acridine (Fig. 3).

The second band in the UPS spectra of compounds **I–II** is due to the ionization processes from three electronic levels (Fig. 3, Table 3). The third band in the spectrum of complex **I** corresponds to three orbitals. The band onset at 11 eV in the spectrum of **I** corresponds to the σ'' MO (Fig. 3, Table 3). The spectrum of compound **II** has a shoulder at 8.9 eV corresponding to the σ''–π orbital and has no band at 10 eV, which is due to the σ' MO.

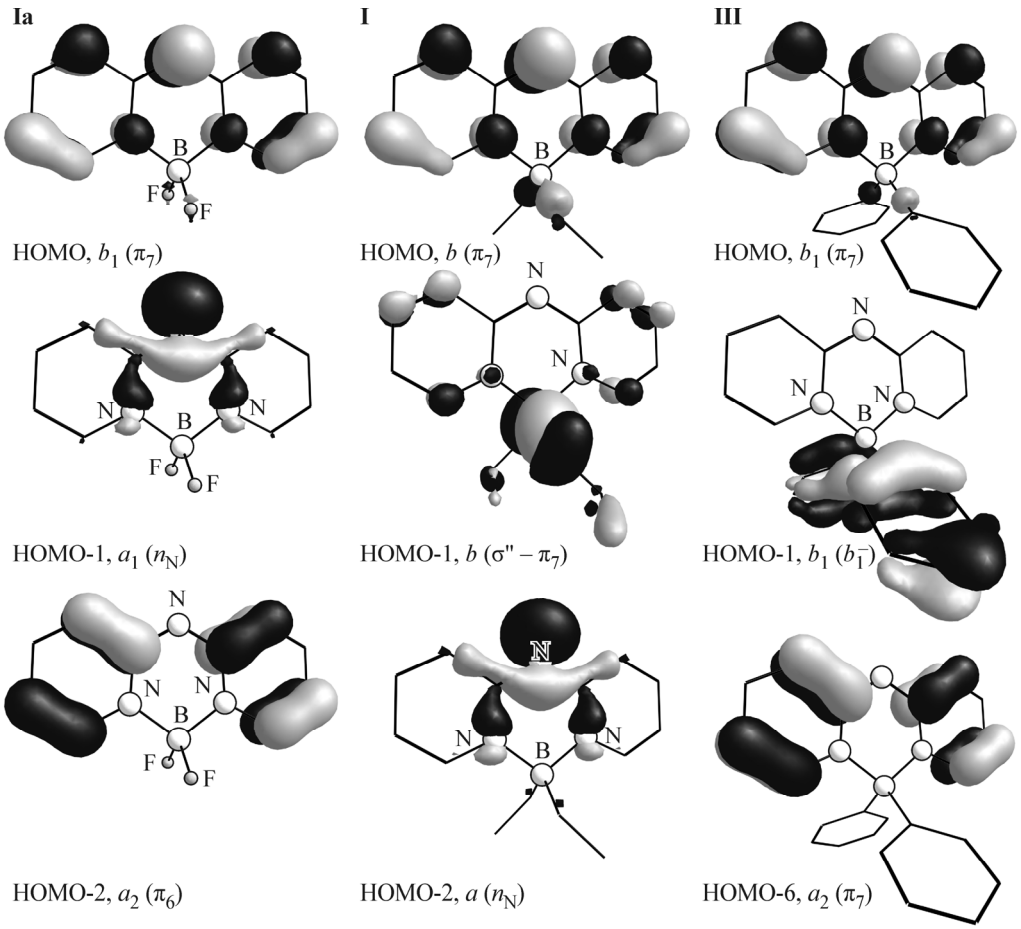

Fig. 2. Shapes of three higher occupied molecular orbitals of complexes **Ia**, **I**, and **III**.

TABLE 4. Correlation of the Symmetry of MOs of Benzene and Phenyl Groups (free and in compounds **III** and **IIIa**)

C_6H_6, D_{6h}	C_6H_5, C_{2v}	$(C_6H_5)_2$	$(C_6H_5)_2$BAA, C_{2v}	C_6H_6, D_{6h}	C_6H_5, C_{2v}	$(C_6H_5)_2$	$(C_6H_5)_2$BAA, C_{2v}
$1e_{1g}(\pi)$	b_1	b_1^-	b_1 (b_1^-)*	$2e_{2g}(\sigma)$	a_1	a_1^-	
		b_1^+	a_1 (b_1^+)			a_1^+	a_1 (a_1^+)
	a_2	a_2^-	a_2 (a_2^-)		b_2	b_2^-	a_2 (b_2^-)
		a_2^+	b_2 (a_2^+)			b_2^+	b_2 (b_2^+)

* "+" denotes the bonding between the C_6H_5 groups, "–" denotes antibonding.

The second band in the spectrum of compound **III** corresponds to seven electronic levels (Fig. 3, Table 3). In the spectrum of **III,** a 8.9 eV peak is due to the photoionization processes from the orbitals localized more on the phenyl groups. In the spectrum of **III,** the energy and intensity of the 8.9 eV peak correlate with the analogous parameters of the first band of **IIIa** corresponding to four orbitals of the phenyl groups and one MO of the chelate ring (Fig. 3). In complex **III**, a –0.57 *e* negative charge of substituents R_2 (Table 2) agrees well with reduced EI values for π electrons of the benzene rings relative to benzene and its substituents [33]. In the spectrum of **III**, a shoulder at 9.4 eV is due to three MOs. The 11 eV region of the spectrum of **III** (Fig. 3) corresponds to the π_5 MO.

For complexes **I**, **II**, and **III**, the maximum difference between the theoretical and experimental energies (the second and third bands), with regard to the average Koopmans defects of 1.96 eV, 2.06 eV, and 2.11 eV, is 0.10 eV (Fig. 3, Table 3).

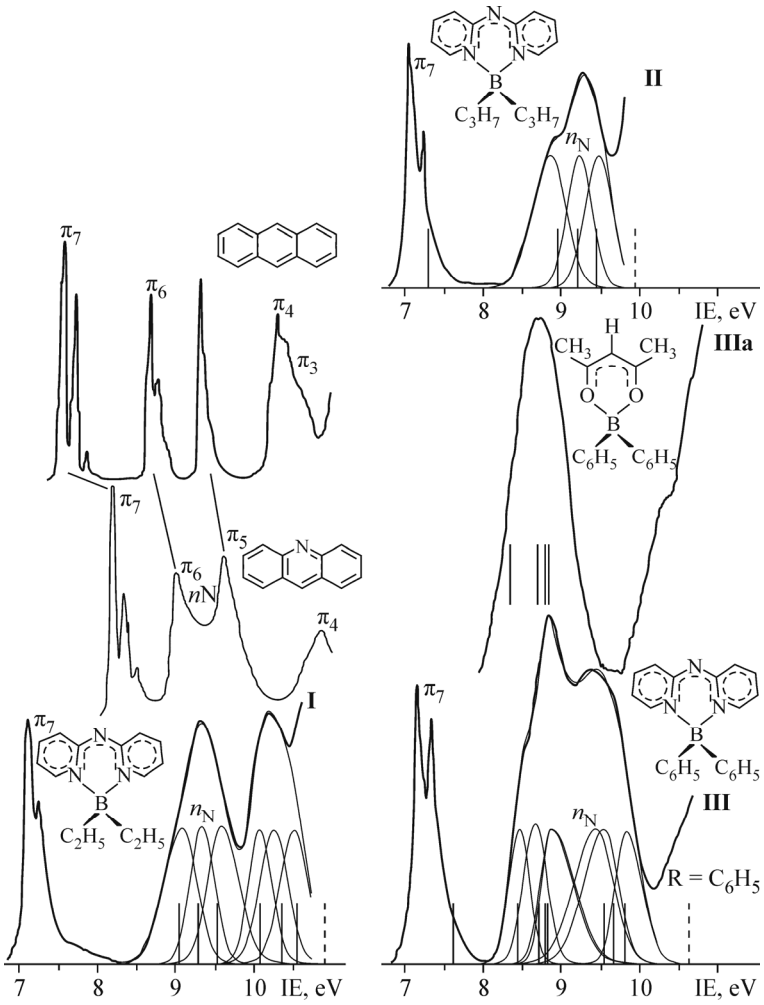

Fig. 3. Photoelectron spectra of anthracene [34], acridine [35], compounds **I–III** and **IIIa** vapor [32]. Based on the calculated data, the bands in the spectra of anthracene and acridine are compared.

The discrepancies between the theoretical IEs ($-\varepsilon_i + \delta_{av}$) for the higher occupied MOs of compounds **I–III** and the experimental IE_1 can be explained by a significant electron density rearrangement when an electron is removed from HOMO.

CONCLUSIONS

The HOMOs of three substituted aza-boron-dipyridomethene correlate with the π_7 orbital of anthracene and acridine, hence, the UPS spectra of the studied compounds have a fine structure of the first band due to the π_7 MO localized on three rings. As opposed to the boron difluoride complex, in the series of the studied compounds the mixing of the chelate ligand π orbitals and pseudo-π MOs of the complexing agent is observed. When ethyl groups at the boron atom are substituted by propyl groups, this does not noticeably change the energies and compositions of six higher occupied MOs. The benzene rings at the boron atom stabilize the levels of the chelate ligand π MO and the σ″–π pseudo-π orbital by 0.1-0.2 eV and 0.7 eV respectively. There is no mixing of the a_2 and b_1 MOs of the benzene rings with the ligand π orbitals in aza-boron-dipyridomethene with phenyl groups at the boron atom and its β-diketonate analogue. In the series of the studied complexes, the maximum discrepancy between the experimental and theoretical IEs is 0.10 eV for 16 electronic levels, which confirms the reliability of the calculated results.

REFERENCES

1. S. A. Tikhonov, V. I. Vovna, N. A. Gelfand, et al., *J. Phys. Chem. A*, **120**, 7361 (2016).
2. E. Giziroglu, A. Nesrullajev, and N. Orhan, *J. Mol. Struct.*, **1056**, 246 (2014).
3. A. Flores-Parra and R. Contreras, *Coord. Chem. Rev.*, **196**, 85 (2000).
4. K. Tanaka, K. Tamashima, A. Nagai, et al., *Macromol.*, **46**, 2969 (2013).
5. S. J. Baker, T. Akama, Y. K. Zhang, et al., *Bioorg. Med. Chem. Lett.*, **16**, 5963 (2006).
6. S. M. Barbon, J. T. Price, P. A. Reinkeluers, and J. B. Gilroy, *Inorg. Chem.*, **53**, 10585 (2014).
7. D. Wang, R. Liu, C. Chen, et al., *Dyes Pigm.*, **99**, 240 (2013).
8. J. H. Gibbs, H. Wang, D. K. Bhupathiraju, et al., *J. Organomet. Chem.*, **798**, 209 (2015).
9. US patent № US 20120037890 A1, F. Okuda, K. Ikeda, T. Sado, T. Ochi, Y. Tanabe, and B. Sawano, *Pyrromethene-Boron Complex Compounds and Organic Electroluminescent Elements Using Same*, I demit su Kosan Co., Lt d. (16.02.2012).
10. S. P. Singh and T. Gayathri, *Eur. J. Org. Chem.*, **22**, 4689 (2014).
11. T. Papalia, G. Siracusano, I. Colao, et al., *Dyes Pigm.*, **110**, 67 (2014).
12. D. Gong, Y. Tian, C. Yang, et al., *Biosens. Bioelectron.*, **85**, 178 (2016).
13. Y. Deng, Y.-Y. Cheng, H. Liu, et al., *Tetrahedron Lett.*, **55**, 3792 (2014).
14. A. Karatay, M. C. Miser, X. Cui, et al., *Dyes Pigm.*, **122**, 286 (2015).
15. A. A. Pakhomov, Y. N. Kononevich, M. V. Stukalova, et al., *Tetrahedron Lett.*, **57**, 979 (2016).
16. S. A. Tikhonov and V. I. Vovna, *J. Struct. Chem.*, **56**, No. 3, 446-453 (2015).
17. S. A. Tikhonov, V. I. Vovna, and A. V. Borisenko, *J. Mol. Struct.*, **1115**, 1 (2016).
18. V. A. Dorokhov, L. I. Lavrinovich, A. S. Shashkov, and B. M. Mikhailov, *Bull. Acad. Sci. USSR, Div. Chem. Sci.*, **30**, 1097 (1981).
19. E. K. U. Gross, E. Runge, and O. Heinonen, *Many Particle Theory*, Adam Hilger (1992).
20. E. N. Economou, *Green's Functions in Quantum Physics*, Springer, New York (1979).
21. S. Hamel, P. Duffy, M. E. Casida, and D. R. Salahub, *J. Electron. Spectrosc. Relat. Phenom.*, **123**, 345 (2002).
22. P. Duffy, D. P. Chong, M. E. Casida, and D. R. Salagub, *Phys. Rev. A*, **50**, 4707 (1994).
23. V. I. Vovna, S. A. Tikhonov, M. V. Kazachek, et al., *J. Electron. Spectrosc. Relat. Phenom.*, **189**, 116 (2013).
24. V. I. Vovna, S. A. Tikhonov, I. B. Lvov, et al., *J. Electron. Spectrosc. Relat. Phenom.*, **197**, 43 (2014).
25. I. S. Osmushko, V. I. Vovna, S. A. Tikhonov, et al., *Int. J. Quantum Chem.*, **116**, 325 (2016).
26. A. A. Granovsky; http://classic.chem.msu.su/gran/firefly/index.html.
27. *Basis Set Exchange*, Version 1.2.2: https://bse.pnl.gov/bse/portal.
28. M. V. Kazachek and I. V. Svistunova, *Spectrochim. Acta, Part A*, **148**, 60 (2015).
29. Y. Kubota, K. Kasatani, H. Takai, et al., *Dalton Trans.*, **44**, 3326 (2015).
30. M.-C. Chang and E. Otten, *Inorg. Chem.*, **54**, 8656 (2015).
31. A. D. Becke, *J. Chem. Phys.*, **98**, 5648 (1993).
32. S. A. Tikhonov, I. B. Lvov, and V. I. Vovna, *Rus. J. Phys. Chem. B*, **8**, 626 (2014).
33. V. I. Nefedov and V. I. Vovna, *Electronic Structure of Organic and Organoelemental Compounds* [in Russian], Nauka, Moscow (1989).
34. T. Kajiwara, S. Masuda, K. Ohno, and Y. Harada, *J. Chem. Soc. Perkin II*, **4**, 507 (1988).
35. J. P. Maier and J.-F. Muller, *Helv. Chim. Acta*, **58**, 1641 (1975).